

The Gould Belt, the de VaucouleursDolidze Belt, and the Orion Arm

V. V. Bobylev^{1,2 0}, A. T. Bajkova¹

¹*Pulkovo Astronomical Observatory, Russian Academy of Sciences,*

²*Sobolev Astronomical Institute, St. Petersburg State University,
Universitetskii pr. 28, Petrodvorets, 198504 Russia*

Based on masers with measured trigonometric parallaxes, we have redetermined the spatial orientation parameters of the Local (Orion) arm. Using 23 sources (the Gould Belt objects were excluded), we have found that their spatial distribution can be approximated by a very narrow ellipsoid elongated in the direction $L_1 = 77.1 \pm 2.9^\circ$ whose symmetry plane is inclined to the Galactic plane at an angle of $5.6 \pm 0.2^\circ$. The longitude of the ascending node of the symmetry plane is $l_\Omega = 70 \pm 3^\circ$. A new estimate for the pitch angle of the Local spiral arm has been obtained by an independent method: $i = 12.9 \pm 2.9^\circ$. Previously, a belt of young B stars, the de Vaucouleurs.Dolidze belt, was pointed out on the celestial sphere with parameters close to such an orientation. We have refined the spatial orientation parameters of this belt based on a homogeneous sample of protostars. The de Vaucouleurs.Dolidze belt can be identified with the Local arm, with the belt proper as a continuous band on the celestial sphere like the Gould Belt being absent due to the peculiarities of the spatial orientation of the Local arm. Using the entire sample of 119 Galactic masers, we have shown that the third axis of their position ellipsoid has no deviation from the direction to the Galactic pole: $B_3 = 89.7 \pm 0.1^\circ$.

DOI: 10.1134/S1063773714120020

Keywords: *masers, Gould Belt, de VaucouleursDolidze belt, Orion arm, local system of stars, Galaxy.*

⁰e-mail: vbobylev@gao.spb.ru

INTRODUCTION

A number of structures consisting of young objects are known in the solar neighborhood: the Gould Belt, de Vaucouleurs–Dolidze belt, the local system of stars, and the Local (Orion) spiral arm. The Gould Belt is the nearest and, hence, best-studied object (Frogel and Stothers 1977; Efremov 1989; Pöppel 1997; Torra et al. 2000). Highly accurate data on the parallaxes and velocities of stars are being gradually accumulated. They allow the spatial characteristics of increasingly distant structures to be refined.

According to present-day estimates, the Gould Belt is a fairly flat system with semiaxes of $350 \times 250 \times 50$ pc, with the direction of its semimajor axis being near $l = 40^\circ$. Its symmetry plane has an inclination to the Galactic plane of about 18° . The longitude of the ascending node is $l_\Omega = 280^\circ$. The Sun is at a distance of ~ 40 pc from the line of nodes. The system’s center lies at a heliocentric distance of ~ 150 pc in the second Galactic quadrant. The estimate of the direction to the center l_0 depends on the sample age from 130° to 180° . The spatial distribution of stars is highly nonuniform: a noticeable drop in density is observed within ≈ 80 pc of the center, i.e., the entire system has the shape of a doughnut. The well-known open cluster α Per with an age of ~ 35 Myr lies near the center of this doughnut. The system of nearby OB associations (de Zeeuw et al. 1999) and open star clusters (Bobylev 2006) belongs to the Gould Belt; a giant neutral hydrogen cloud called the Lindblad Ring (Lindblad 1967, 2000) is associated with it.

As was pointed out by Pöppel (2001), it can be said with confidence that only relatively nearby stars with a spectral type no later than B2.5 belong to the Gould Belt. However, the Hipparcos trigonometric parallaxes with a relative error of less than 10% allow only a small solar neighborhood with a radius of ~ 120 pc to be analyzed.

The parameters of the de Vaucouleurs–Dolidze belt are known very approximately. According to Figs. 1 and 2 from Dolidze (1980), the inclination of its symmetry plane to the Galactic plane ranges from 16° (from young B stars) to 44° (from supernova remnants). Since the distances to the objects were not known, with the exception of a few β Cep stars, the parameters were determined exclusively from the distribution of stars on the celestial sphere. This belt reaches the greatest elevation above the Galactic plane in a direction $l \approx 120^\circ$. Dolidze called this belt the de Vaucouleurs belt and considered it to be part of the Local spiral arm, a structure as close to the Sun as the Gould Belt. De Vaucouleurs (1954) believed that the stars he identified belonged to the bridge between the Galaxy and the Magellanic Clouds, the Magellanic Stream. We now know that he was wrong, because the Magellanic Stream consists of hydrogen clouds and no stars have been detected in it.

Olano (2001) identified the local system of stars with the Local (Orion) arm and investigated the evolution of this structure with a mass of $\sim 2 \times 10^7 M_\odot$ over the last 100 Myr by numerical simulations. According to Olano’s model, there was a high initial velocity (≈ 50 km s $^{-1}$) of the gas from which the local system was formed. It is suggested that such a velocity could be reached as a result of the interaction with the Carina–Sagittarius arm. The collision of the gas cloud with the spiral density wave led to its fragmentation. In this model, such clusters as the Hyades, the Pleiades, Coma Berenices, and the Sirius cluster, are considered as the debris of a once single complex, while contraction of the central regions of the parent cloud gave rise to the Gould Belt.

As analysis of various data shows, the large-scale spiral pattern in the Galaxy can be described either by the two-armed logarithmic spiral model with a constant pitch angle of about 6° or by the four-armed model with a pitch angle of $12 - 13^\circ$ (Efremov 2011; Vall L ee

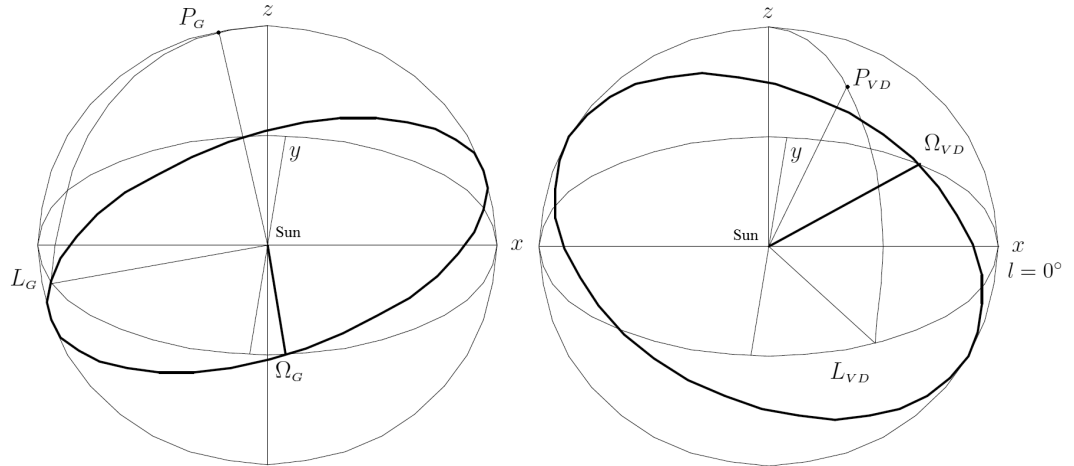


Figure 1: Orientation of the great circles on the celestial sphere associated with the Gould Belt (on the left) and the de Vaucouleurs–Dolidze belt (on the right) relative to the rectangular Galactic coordinate system.

2014; Bobylev and Bajkova 2014; Hou and Han 2014), with many authors giving preference to the four-armed model. In their recent paper, Hou and Han (2014) provide arguments for a slightly more complex model: in their opinion, the four-armed model with a variable pitch angle (a polynomial–logarithmic model) is in even better agreement with the available data. The Orion arm (Efremov 2011; Xu et al. 2013) is not a fully-fledged spiral arm. It is a spur (a small branch) of either the Carina–Sagittarius arm or the Perseus arm (Hou and Han 2014). In this paper, we hold this viewpoint.

The orientation of the great circles on the celestial sphere associated with the Gould Belt and the de Vaucouleurs–Dolidze belt is schematically shown in Fig. 1. The coordinates of the pole of the great circle L, B and the longitude of the ascending node Ω are marked on each graph.

At present, the masers with their trigonometric parallaxes measured by VLBI (Xu et al. 2013; Reid et al. 2014) provide an unprecedented possibility for studying objects in the Local spiral arm. The relative error in determining the parallaxes by this method is, on average, less than 10%. There are about ten such masers in the Gould Belt, which is not very many. However, their number in the Local spiral arm is already 37, which allows a thorough three-dimensional analysis of this system to be performed. The goal of this paper is to redetermine the spatial orientation parameters of the Local arm using data on the positions of masers.

THE METHOD

We apply the well-known method of determining the symmetry plane of a stellar system with respect to the principal (in our case, Galactic) coordinate system. The basics of the approach were outlined by Polak (1935); its description can be found in the book by Trumpler and Weaver (1953). The technique for estimating the errors in the angles is presented in Parenago (1951) and Pavlovskaya (1971). Recently, this method was applied to determine the orientation parameters of the Cepheid system in the Galaxy (Bobylev 2013).

In the rectangular coordinate system centered on the Sun, the x axis is directed toward the Galactic center, the y axis is in the direction of Galactic rotation ($l=90^\circ$, $b=0^\circ$), and the z axis is directed toward the North Galactic Pole. Then,

$$\begin{aligned}x &= r \cos l \cos b, \\y &= r \sin l \cos b, \\z &= r \sin b.\end{aligned}\tag{1}$$

Let m , n , and k be the direction cosines of the pole of the sought-for great circle from the x , y , and z axes. The sought-for symmetry plane of the stellar system is then determined as the plane for which the sum of the squares of the heights, $h = mx + ny + kz$, is at a minimum:

$$\sum h^2 = \min.\tag{2}$$

The sum of the squares

$$h^2 = x^2m^2 + y^2n^2 + z^2k^2 + 2yznk + 2xzk m + 2xymn\tag{3}$$

can be designated as $2P = \sum h^2$. As a result, the problem is reduced to searching for the minimum of the function P :

$$2P = am^2 + bn^2 + ck^2 + 2f nk + 2ekm + 2dmn,\tag{4}$$

where the second-order moments of the coordinates $a = [xx]$, $b = [yy]$, $c = [zz]$, $f = [yz]$, $e = [xz]$, $d = [xy]$, written via the Gauss brackets, are the components of a symmetric tensor:

$$\begin{pmatrix} a & d & e \\ d & b & f \\ e & f & c \end{pmatrix},\tag{5}$$

whose eigenvalues $\lambda_{1,2,3}$ are found from the solution of the secular equation

$$\begin{vmatrix} a - \lambda & d & e \\ d & b - \lambda & f \\ e & f & c - \lambda \end{vmatrix} = 0,\tag{6}$$

while the directions of the principal axes $L_{1,2,3}$ and $B_{1,2,3}$ are found from the relations

$$\tan L_{1,2,3} = \frac{ef - (c - \lambda)d}{(b - \lambda)(c - \lambda) - f^2},\tag{7}$$

$$\tan B_{1,2,3} = \frac{(b - \lambda)e - df}{f^2 - (b - \lambda)(c - \lambda)} \cos L_{1,2,3}.\tag{8}$$

The errors in $L_{1,2,3}$ and $B_{1,2,3}$ are estimated according to the following scheme:

$$\varepsilon(L_2) = \varepsilon(L_3) = \frac{\varepsilon(\overline{xy})}{a - b},\tag{9}$$

$$\varepsilon(B_2) = \varepsilon(\varphi) = \frac{\varepsilon(\overline{xz})}{a - c},\tag{10}$$

$$\varepsilon(B_3) = \varepsilon(\psi) = \frac{\varepsilon(\overline{yz})}{b - c},\tag{11}$$

$$\varepsilon^2(L_1) = \frac{\varphi^2 \cdot \varepsilon^2(\psi) + \psi^2 \cdot \varepsilon^2(\varphi)}{(\varphi^2 + \psi^2)^2}, \quad (12)$$

$$\varepsilon^2(B_1) = \frac{\sin^2 L_1 \cdot \varepsilon^2(\psi) + \cos^2 L_1 \cdot \varepsilon^2(L_1)}{(\sin^2 L_1 + \psi^2)^2}, \quad (13)$$

where

$$\varphi = \cot B_1 \cdot \cos L_1, \quad \psi = \cot B_1 \cdot \sin L_1, \quad (14)$$

The three quantities $\overline{x^2 y^2}$, $\overline{x^2 z^2}$ and $\overline{y^2 z^2}$ should be calculated in advance. Then,

$$\varepsilon^2(\overline{xy}) = (\overline{x^2 y^2} - d^2)/n, \quad (15)$$

$$\varepsilon^2(\overline{xz}) = (\overline{x^2 z^2} - e^2)/n, \quad (16)$$

$$\varepsilon^2(\overline{yz}) = (\overline{y^2 z^2} - f^2)/n, \quad (17)$$

where n is the number of stars. Thus, the algorithm for solving the problem consists in (i) setting up the function $2P$ (4), (ii) seeking for the roots of the secular equation (6), and (iii) estimating the directions of the principal axes of the position ellipsoid from Eqs. (7)–(17). In the classical case, the problem was solved for a unit sphere ($r = 1$), but here we propose to use the distances that play the role of weights. As can be seen from Eqs. (13), the errors in the directions L_2 and L_3 coincide; the errors in all the remaining directions are calculated independently of one another.

DATA

The Sample of Masers

Based on published data, we gathered information about the coordinates, line-of-sight velocities, proper motions, and trigonometric parallaxes of Galactic masers measured by VLBI with an error, on average, less than 10%. These masers are associated with very young objects, protostars of mostly high masses located in regions of active star formation. The proper motions and trigonometric parallaxes of the masers are absolute, because they are determined with respect to extragalactic reference objects (quasars).

One of the projects to measure the trigonometric parallaxes and proper motions is the Japanese VERA (VLBI Exploration of Radio Astrometry) project devoted to the observations of H₂O masers at 22.2 GHz (Hirota et al. 2007) and a number of SiO masers (which are very few among young objects) at 43 GHz (Kim et al. 2008).

Methanol (CH₃OH, 6.7 and 12.2 GHz) and H₂O masers are observed in the USA on VLBA (Reid et al. 2009). Similar observations are also being carried out within the framework of the European VLBI network (Rygl et al. 2010), in which three Russian antennas are involved: Svetloe, Zelenchukskaya, and Badary. These two programs enter into the BeSSeL project¹ (Bar and Spiral Structure Legacy Survey, Brunthaler et al. 2011).

The VLBI observations of radio stars in continuum at 8.4 GHz are being carried out with the same goals (Torres et al. 2009; Dzib et al. 2011). Radio sources located in the Local arm associated with young low-mass protostars are observed within the framework of this program.

¹<http://www3.mpifr-bonn.mpg.de/staff/abrunthaler/BeSSeL/index.shtml>

Reid et al. (2014) gave a summary of the measurements of the trigonometric parallaxes, proper motions, and line-of-sight velocities for 103 masers. Six more sources of the Local arm from the list by Xu et al. (2013), EC 95, L 1448C, S1, DoAr21, SVC13/NGC1333, and IRAS 16293.2422, two red supergiants, PZ Cas (Kusuno et al. 2013) and IRAS 22480+6002 (Imai et al. 2012), and, finally, IRAS 22555+6213 (Chibueze et al. 2014), Cyg X-1 (Reid et al. 2011), IRAS 20143+3634 (Burns et al. 2014) as well as five low-mass nearby radio stars in Taurus, Hubble 4 and HDE 283572 (Torres et al. 2007), T Tau N (Loinard et al. 2007), HP Tau/G2 (Torres et al. 2009), and V773 Tau (Torres et al. 2012), can be added to these data; they all belong to the Local arm.

According to Reid et al. (2014), the source G176.51+00.20 with coordinates $(x, y, z) = (-0.96, 0.05, 0.0)$ kpc may belong to the Local arm. However, since it deviates greatly from the general distribution, we did not include it in the list of masers from the Local arm. Thus, a total of 37 masers belong to the Local arm. The entire sample contains 119 sources.

The Sample of O–B2.5 Stars

The sample of selected 200 massive (more than $10M_{\odot}$) O–B2.5 stars is described in detail in Bobylev and Bajkova (2013). It contains spectroscopic binary O stars with well-determined kinematic characteristics within ~ 3 kpc of the Sun. This sample also includes 124 stars from the Hipparcos catalogue (van Leeuwen 2007) with spectral types from B0 to B2.5 whose parallaxes were determined with a relative error of no less than 10% and for which the line-of-sight velocities are known. From this database we selected 161 stars within 0.7 kpc of the Sun. As was shown by Bobylev and Bajkova (2013), almost all of them belong to the Gould Belt.

RESULTS AND DISCUSSION

Initially, we tested the method on Gould Belt stars. Based on a sample of 161 O–B2.5, we found

$$\begin{aligned} L_1 &= 59 \pm 12^\circ, & B_1 &= 12 \pm 2^\circ, \\ L_2 &= 148 \pm 4^\circ, & B_2 &= -5 \pm 1^\circ, \\ L_3 &= 216 \pm 4^\circ, & B_3 &= 77 \pm 1^\circ. \end{aligned} \tag{18}$$

The principal semiaxes of the ellipsoid in our method are determined to within a constant and their ratios are $\lambda_1 : \lambda_2 : \lambda_3 = 1 : 0.78 : 0.22$. If the size of the first semiaxis is taken to be 350 pc, then the ellipsoid will have sizes, 350 272 78 pc, similar to those of the Lindblad Ring. In contrast to the Lindblad hydrogen Ring whose geometric center lies in the second quadrant, we obtained slightly different coordinates of the geometric center of the “stellar” ellipsoid: $x_0 = -35 \pm 13$ pc, $y_0 = -92 \pm 14$ pc, and $z_0 = -22 \pm 5$ pc. Obviously, quite a few stars from the Scorpius–Centaurus association (a dense cloud of points in the fourth quadrant in Fig. 2) exert a great influence on the calculation of these coordinates. Even if we take the stars from the Scorpius–Centaurus association with smaller weights, the geometric center of their distribution will be in the third quadrant. A similar situation with the geometric center of the Gould Belt determined from open star clusters was pointed out by Piskunov et al. (2006). In this case, the parameters of the kinematic center of the Gould Belt determined from stars are $l_0 = 160^\circ$ and $R_0 = 150$ pc (Bobylev et al. 2004).

On the whole, the parameters found are in good agreement with the results of determining the orientation of the Gould Belt from various samples. As can be seen from solution

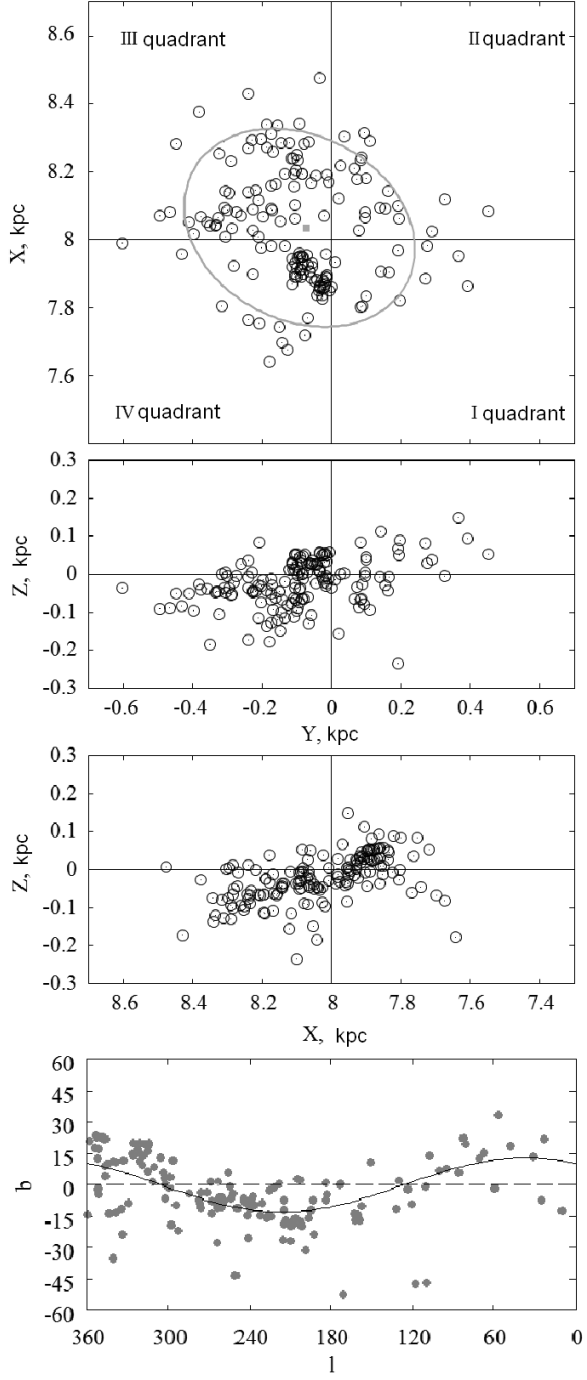


Figure 2: Positions of 161 O–B2.5 stars in projection onto the Galactic XY , YZ and XZ planes. The upper panel displays the ellipse found and the square marks its center; the lower panel presents the apparent distribution of these stars on the celestial sphere.

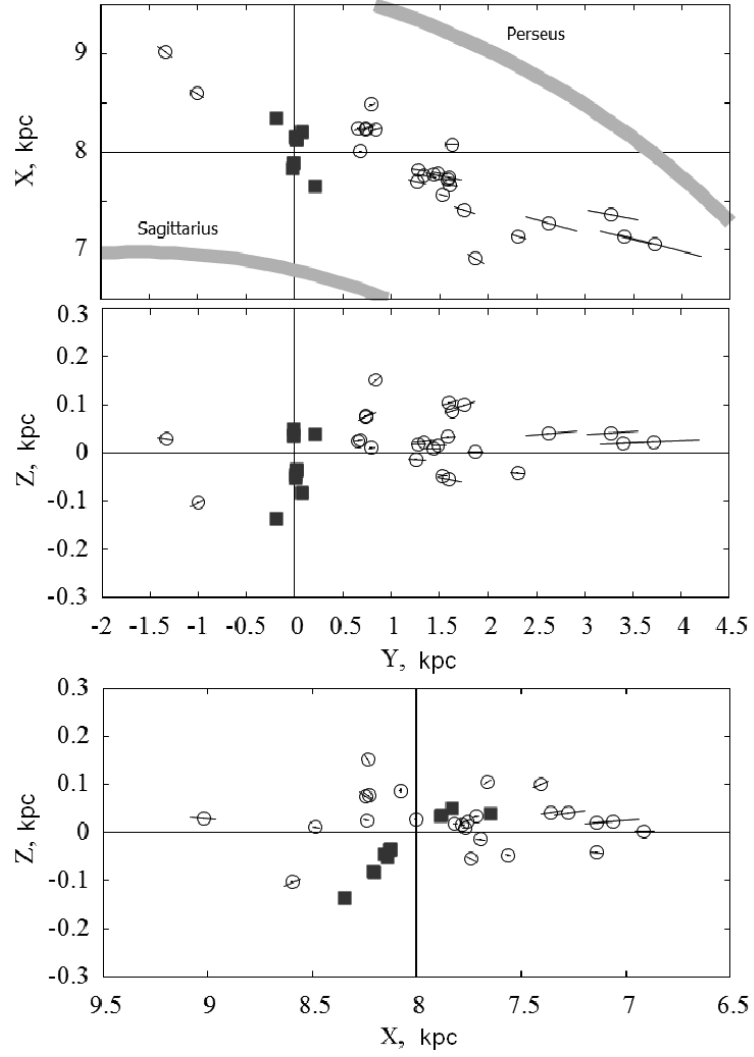


Figure 3: Positions of Local-arm masers in projection onto the XY , YZ and XZ planes. The bars denote the distance errors; the Gould-Belt masers are marked by the dark squares. Fragments of the four-armed spiral pattern constructed with the pitch angle $i = 13^\circ$ are presented on the upper panel.

(18), the orientation of the third axis L_3, B_3 is essentially the same as that in Fig. 1, the inclination to the Galactic plane is $13 \pm 1^\circ$, and the longitude of the ascending node is $l_\Omega = L_3 + 90^\circ = 306 \pm 4^\circ$. Having analyzed a large sample of Hipparcos OB stars, Torra et al. (2000) determined the inclination to the Galactic plane, $16^\circ - 22^\circ$, and the longitude of the ascending node, $l_\Omega = 275^\circ - 295^\circ$.

The positions of 161 O–B2.5 stars in projection onto the Galactic XY, YZ and XZ planes as well as their Galactic coordinates l and b are presented in Fig. 2. We denoted the X, Y and Z axes by big letters, with the X axis being directed away from the Galactic center. We took the solar Galactocentric distance to be $R_0 = 8$ kpc. The sine wave that corresponds to the parameters (18) found is plotted on the lower panel. As can be seen from the figure, the stars that we selected by their spectral type and relative parallax error and that satisfy the constraints on their coordinates $r \leq 0.7$ kpc and $y \leq 0.5$ kpc excellently trace the Gould Belt; they are even distributed in the form of a doughnut. This picture is very similar to the distribution of neutral hydrogen, the Lindblad Ring. We can conclude that the method of analysis being applied works and yields good results. Unfortunately, so far there are only 12 masers and they are concentrated only in six regions associated specifically with the Gould Belt, but the orientation parameters cannot be found by the described method from such a small number of sources.

Using 37 masers, we found the following directions of the principal axes of the position ellipsoid:

$$\begin{aligned} L_1 &= 76.0 \pm 0.2^\circ, & B_1 &= 0.7 \pm 0.0^\circ, \\ L_2 &= 166.0 \pm 2.5^\circ, & B_2 &= 1.2 \pm 0.3^\circ, \\ L_3 &= 313.3 \pm 2.5^\circ, & B_3 &= 88.6 \pm 0.1^\circ. \end{aligned} \quad (19)$$

If we remove the Gould Belt masers ($r < 0.5$ kpc) and the two stars from the third quadrant that slightly spoil the solution, then from the remaining 23 masers of the Local arm we will have

$$\begin{aligned} L_1 &= 77.1 \pm 0.1^\circ, & B_1 &= 0.7 \pm 0.0^\circ, \\ L_2 &= 167.1 \pm 2.9^\circ, & B_2 &= 5.6 \pm 0.1^\circ, \\ L_3 &= 340.0 \pm 2.9^\circ, & B_3 &= 84.4 \pm 0.2^\circ. \end{aligned} \quad (20)$$

The derived ellipsoid is highly elongated; it has the axis ratios $\lambda_1 : \lambda_2 : \lambda_3 = 1 : 0.15 : 0.02$. If, for example, the half-width of the Local arm is taken, according to the estimate by Reid et al. (2014), to be 0.33 kpc (this is the size of the second semiaxis λ_2), then the ellipsoid found will have the sizes $2.15 \times 0.33 \times 0.05$ kpc. If we take into account the fact that the geometric center of the Local arm is shifted toward the Galactic anticenter by ~ 0.5 kpc, then the derived ellipsoid is a pretty good approximation of the distribution of masers in Fig. 3 and OB associations of the Local arm in Fig. 4. The longitude of the ascending node of the symmetry plane is $l_\Omega = 70 \pm 3^\circ$.

The pitch angle of the spiral pattern is easily estimated via the direction of the first axis L_1 , $i = 90^\circ - L_1 = 12.9 \pm 2.9^\circ$. Here, when estimating the error in the angle i , we take the largest of the errors in the longitudes. Solution (19) obtained from all sources of the Local arm is also suitable for finding the pitch angle, then $i = 14.0 \pm 2.5^\circ$. Both these values are in good agreement with the estimate from Xu et al. (2013), where it was determined from the data on 30 masers in the Local arm, $i = 10.1 \pm 2.7^\circ$. Note once again that we consider the Local arm to be a spur. However, the value of $i = 12.9 \pm 2.9^\circ$ found shows that the Local arm is parallel to two spiral arm segments belonging to the large-scale structure of the Galaxy, between the Perseus and Carina. Sagittarius arms. In our opinion, such a position suggests that the Local arm was formed under the action of the Galactic spiral density wave.

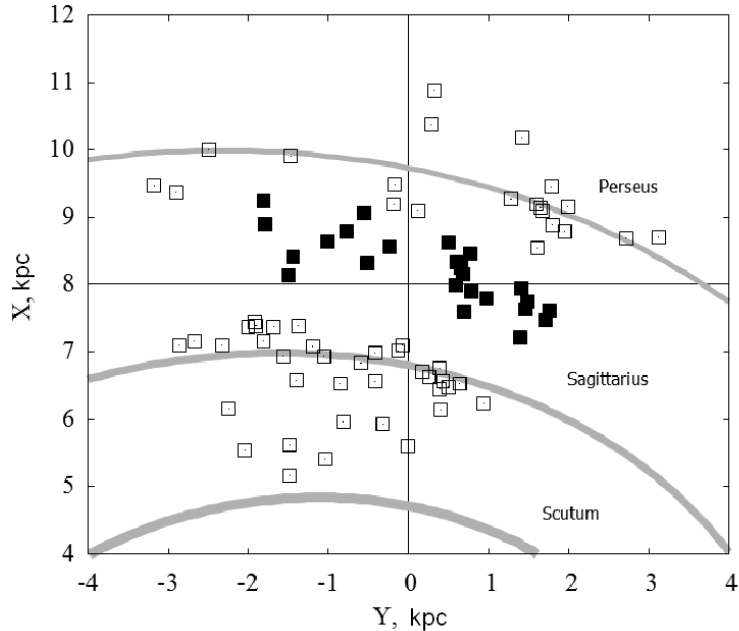


Figure 4: Positions of OB associations (from Melnik and Dambis 2009) in projection onto the Galactic XY plane. The associations tracing the Local arm are marked by the dark squares (the Gould-Belt associations were excluded).

Note that the pitch angle found by Hou and Han (2014) for the Local arm, $i = 1^\circ - 3^\circ$, differs significantly from our result as well as from the result of Xu et al. (2013).

Figure 3 presents the positions of Local-arm masers in projection onto the XY , YZ , and XZ planes. To construct the figure, we took the solar Galactocentric distance $R_0 = 8$ kpc; the positions of three segments of the Perseus and Carina–Sagittarius spiral arms are plotted for this value based on the data from Bobylev and Bajkova (2014). An inclination of the Gould Belt to the X axis of about $+14^\circ$ and an inclination of the more distant Local arm masers of about -6° (this projection resembles Fig. 1) are clearly seen in the distribution of masers on the XZ plane (the lower panel in Fig. 3).

Finally, from all the available 119 Galactic masers we find

$$\begin{aligned}
 L_1 &= 34.5 \pm 0.0^\circ, & B_1 &= 0.1 \pm 0.0^\circ, \\
 L_2 &= 124.5 \pm 6.9^\circ, & B_2 &= 0.3 \pm 0.0^\circ, \\
 L_3 &= 295.5 \pm 6.9^\circ, & B_3 &= 89.7 \pm 0.1^\circ.
 \end{aligned}
 \tag{21}$$

We see that, to within the determination error, the third axis B_3 is directed exactly to the Galactic pole. The nonzero value of the first axis L_1 only suggests that the distribution of masers in the Galactic XY plane is asymmetric (the empty fourth quadrant) due to the absence of observations from the Earth's Southern Hemisphere.

Consider the question of whether the de Vaucouleurs–Dolidze belt exists like the Gould Belt or this is something else. For this purpose, it is first necessary to look at the distribution of Local-arm objects on the celestial sphere. As can be seen from Fig. 3, there are no masers in the third Galactic quadrant. To fill this gap, we invoked the data on well-known OB associations with reliable distance estimates. These associations are shown in Fig. 4. To construct this figure, we used the data of Table 1 from Melnik and Dambis (2009), where the

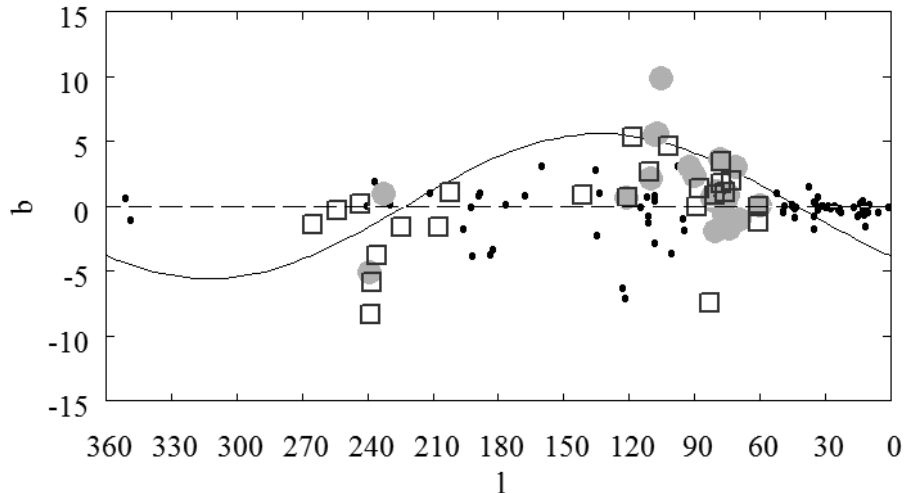


Figure 5: Apparent positions of masers and OB associations on the celestial sphere. The Local-arm masers are marked by the big gray circles, the distant Galactic masers that do not belong to the Local arm are marked by the filled circles, and the OB associations of the Local arm are denoted by the open squares.

distances reconciled with the Cepheid scale are given. A similar, in principle, picture can also be seen in Fig. 10 from Melnik and Efremov (1995), where a slightly different distance scale was used.

Note that the distribution of associations in the segments of the Perseus and Carina.Sagittarius spiral arms in Fig. 4 agrees excellently with the four-armed spiral pattern with the pitch angle $i = 13^\circ$ plotted according to Bobylev and Bajkova (2014). The question about the number of spiral arms in the Galaxy has not yet been solved completely. A detailed discussion of this question can be found in a recent paper by Hou and Han (2014), who used the latest extensive data on traces of the Galactic spiral structure: neutral and ionized hydrogen, giant molecular clouds, and masers.

The apparent distribution of Local-arm masers and OB associations on the celestial sphere is presented in Fig. 5, all of the remaining Galactic masers are also shown, and the sine wave constructed according to solution (20) is plotted. As can be seen from the figure, the distant masers lie very close to the Galactic plane toward the Galactic center, but there are many sources in a direction near $l = 80^\circ$ and they have fairly large elevations. In this direction, one of the OB associations deviates greatly from the general distribution, possibly because of the large distance measurement error. This association is Cyg OB4 ($r = 0.8$ kpc). It is most likely slightly nearer and is associated with the Gould Belt. All of the remaining associations in this direction lie very close together, in good agreement with the positions of Local-arm masers. In a direction near $l = 250^\circ$, the positions of OB associations excellently complement the overall picture.

It can be seen from Fig. 5 that there are two clumps of Local-arm objects near $l = 77^\circ$ and in the diametrically opposite direction $l = 257^\circ$. The remaining space along the plotted sine wave is empty. Therefore, the de Vaucouleurs-Dolidze belt proper as a continuous band on the celestial sphere like the Gould Belt is simply absent. There is the Local arm. Its spatial location relative to the Sun is such that we observe its two projections as two dense clumps of stars in the directions $l = 77^\circ$ and $l = 257^\circ$. Moreover, when we separate the

Gould Belt as an independent structure, we just cannot see quite a few Local-arm masers or OB associations in the direction of the second axis of the Local arm $l = 167 - 347^\circ$, given the narrowness of the Local arm, because there are none of them.

It is important to note the following. The deviation of the systems symmetry plane from the Galactic plane means that some forces cause the stars to rise/sink in the vertical direction. Studying the velocities of stars is of great interest in this regard. Such vertical oscillations are known for the velocities of Gould-Belt stars. There is even the term vertical oscillation axis (Comerón 1999; Lindblad 2000). It is interesting to check the velocities of Local-arm stars, especially those in the first and second quadrants, where the stars reach considerable heights (Fig. 4). However, this is the objective of our next paper.

CONCLUSIONS

Based on published data, we gathered information about the Galactic masers with their trigonometric parallaxes measured by VLBI. The sources located in the Local arm are of greatest interest for this work. To determine the spatial orientation of this system, we applied the well-known method of three-dimensional analysis that consists in determining the parameters of the position ellipsoid.

Initially, the method was tested on Gould-Belt stars. For this purpose, we used a sample of 161 O–B2.5 stars whose distances are known with errors of no less than 10–15%. The determined orientation parameters of the Gould Belt system were shown to be in good agreement with the results of other authors.

Using 23 masers (the Gould-Belt objects were excluded) from the Local arm, we found that their spatial distribution could be approximated by a very narrow ellipsoid elongated in the direction $L_1 = 77.1 \pm 2.9^\circ$ whose symmetry plane is inclined to the Galactic plane at an angle of $5.6 \pm 0.2^\circ$. The longitude of the ascending node of the symmetry plane is $l_\Omega = 70 \pm 3^\circ$.

The orientation of the first axis L_1 allows a new estimate for the pitch angle of the spiral pattern to be obtained for the Local arm, $i = 12.9 \pm 2.9^\circ$. This value shows that the Local arm is parallel to two spiral arm segments belonging to the large-scale structure of the Galaxy, between the Perseus and Carina. Sagittarius arms. In our opinion, this position suggests that the Local arm was formed under the action of the Galactic spiral density wave.

Previously, the de Vaucouleurs–Dolidze stellar belt with parameters close to such an orientation was known on the celestial sphere. In this paper, we refined significantly the spatial orientation parameters of this belt based on a very homogeneous sample of protostars. The results obtained lead to the conclusion that we can identify the de Vaucouleurs–Dolidze belt with two dense clumps of stars in the directions $l = 77^\circ$ and $l = 257^\circ$ that do not contain any Gould-Belt objects, with the de Vaucouleurs–Dolidze belt proper as a continuous band on the celestial sphere like the Gould Belt being simply absent.

The main conclusion of our analysis is as follows. If the Local arm is considered as a whole, then the third axis of the position ellipsoid has an insignificant deviation from the Galactic z axis, as can be seen from solution (19). If, however, the Gould Belt and the rest of the Local arm are considered separately, then the position ellipsoid for each of these parts has a significantly different orientation, solutions (18) and (20).

Using the entire sample of 119 masers, we showed that the third axis of their position ellipsoid has no significant deviation from the direction to the Galactic pole.

ACKNOWLEDGMENTS

We are grateful to the referee for the useful remarks that contributed to an improvement of the paper. This work was supported by the Nonstationary Phenomena in Objects of the Universe Program P-21 of the Presidium of the Russian Academy of Sciences.

REFERENCES

1. V. V. Bobylev, *Astron. Lett.* 30, 159 (2004).
2. V. V. Bobylev, *Astron. Lett.* 32, 816 (2006).
3. V. V. Bobylev and A. T. Bajkova, *Astron. Lett.* 39, 532 (2013).
4. V. V. Bobylev, *Astron. Lett.* 39, 753 (2013).
5. V. V. Bobylev and A. T. Bajkova, *Mon. Not. R. Astron. Soc.* 437, 1549 (2014).
6. A. Brunthaler, M. J. Reid, K. M. Menten, X.-W. Zheng, A. Bartkiewicz, Y. K. Choi, T. Dame, K. Hachisuka, K. Immer, G. Moellenbrock, et al., *Astron. Nach.* 332, 461 (2011).
7. R. A. Burns, Y. Yamaguchi, T. Handa, T. Omodaka, T. Nagayama, A. Nakagawa, M. Hayashi, T. Kamezaki, J. O. Chibueze, et al., arXiv:1404.5506 (2014).
8. J. O. Chibueze, H. Sakanoue, T. Nagayama, T. Omodaka, T. Handa, T. Kamezaki, R. Burns, H. Kobayashi, H. Nakanishi, M. Honma, et al., arXiv:1406.277 (2014).
9. F. Comer . on, *Astron. Astrophys.* 351, 506 (1999).
10. M. V. Dolidze, *Sov. Astron. Lett.* 6, 394 (1980).
11. S. Dzib, L. Loinard, L. F. Rodriguez, A. J. Mioduszewski, and R. M. Torres, *Astrophys. J.* 733, 71 (2011).
12. Yu.N. Efremov, *Sites of Star Formation in Galaxies* (Nauka, Moscow, 1989) [in Russian].
13. Yu. N. Efremov, *Astron.Rep.* 55, 108 (2011).
14. J. A. Frogel and R. Stothers, *Astron. J.* 82, 890 (1977).
15. T. Hirota, T. Bushimata, Y. K. Choi, M. Honma, H. Imai, K. Iwadate, T. Jike, S. Kamenoi, O. Kameya, R. Kamohara, et al., *Publ. Astron. Soc. Jpn.* 59, 897 (2007).
16. L. G. Hou and J. L. Han, arXiv:1407.7331 (2014).
17. H. Imai, N. Sakai, H. Nakanishi, H. Sakanoue, M. Honma, and T. Miyaji, *Publ. Astron. Soc. Jpn.* 64, 142 (2012).
18. M. K. Kim, T. Hirota, M. Honma, H. Kobayashi, T. Bushimata, Y. K. Choi, H. Imai, K. Iwadate, T. Jike, S. Kamenoi, et al., *Publ. Astron. Soc. Jpn.* 60, 991 (2008).
19. K. Kusuno, Y. Asaki, H. Imai, and T. Oyama, *Astrophys. J.* 774, 107 (2013).
20. F. van Leeuwen, *Hipparcos, the New Reduction of the Raw Data* (Springer, Dordrecht, 2007).
21. P. O. Lindblad, *Bull. Astron. Inst. Netherland* 19, 34 (1967).
22. P. O. Lindblad, *Astron. Astrophys.* 363, 154 (2000).
23. L. Loinard, R. M. Torres, A. J. Mioduszewski, L. F. Rodriguez, R. A. Gonzalez-Lopezlira, R. Lachaume, V. Vazquez, and E. Gonzalez, *Astrophys. J.* 671, 546 (2007).
24. A.M.Melnik and Yu. N. Efremov, *Astron. Lett.* 21, 10 (1995).
25. A. M. Melnik, and A. K. Dambis, *Mon. Not. R. Astron. Soc.* 400, 518 (2009).
26. C. A. Olano, *Astron. Astrophys.* 121, 295 (2001).
27. P. P. Parenago, *Tr. Gos. Astron. Inst. Shternberga* 20, 26 (1951).

28. E. D. Pavlovskaya, Practical Works on Stellar Astronomy, Ed. by P. G. Kulikovskii (Nauka, Moscow, 1971), p. 162 [in Russian].
29. A. E. Piskunov, N. V. Kharchenko, S. R'oser, E. Schilbach, and R.-D. Scholz, *Astron. Astrophys.* 445, 545 (2006).
30. I. F. Polak, Introduction to Stellar Astronomy (ONTI, Moscow, Leningrad, 1935) [in Russian].
31. W. G. L. P . oppel, *Fundament. Cosm. Phys.* 18, 1 (1997).
32. W. G. L. P . oppel, *ASP Conf. Ser.* 243, 667 (2001).
33. M. J. Reid, K. M. Menten, X. W. Zheng, A. Brunthaler, L. Moscadelli, Y. Xu, B. Zhang, M. Sato, M. Honma, T. Hirota, et al., *Astrophys. J.* 700, 137 (2009).
34. M. J. Reid, J. E. McClintock, R. Narayan, L. Gou, R. A. Remillard, and J. A. Orosz, *Astrophys. J.* 742, 83 (2011).
35. M. J. Reid, K. M. Menten, A. Brunthaler, X.W. Zheng, T.M. Dame, Y. Xu, Y.Wu, B. Zhang, A. Sanna, M. Sato, et al., *Astrophys. J.* 783, 130 (2014).
36. K. L. J. Rygl, A. Brunthaler, M. J. Reid, K. M. Menten, H. J. van Langevelde, and Y. Xu, *Astron. Astrophys.* 511, A2 (2010).
37. J. Torra, D. Fernandez, and F. Figueras, *Astron. Astrophys.* 359, 82 (2000).
38. R. M. Torres, L. Loinard, A. J. Mioduszewski, and L. F. Rodriguez, *Astrophys. J.* 671, 1813 (2007).
39. R. M. Torres, L. Loinard, A. J. Mioduszewski, and L. F. Rodriguez, *Astrophys. J.* 698, 242 (2009).
40. R. M. Torres, L. Loinard, A. J. Mioduszewski, A. F. Boden, R. Franco-Hernandez, W. H. T. Vlemmings, and L. F. Rodriguez, *Astrophys. J.* 747, 18 (2012).
41. R. J. Trumpler and H. F. Weaver, *Statistical Astronomy* (Univ. California Press, Berkely, 1953).
42. J. P. Vall . ee, *Mon. Not. R. Astron. Soc.* 442, 2993 (2014).
43. G. de Vaucouleurs, *Observatory* 74, 23 (1954).
44. Y. Xu, J. J. Li, M. J. Reid, K. M. Menten, X. W. Zheng, A. Brunthaler, L. Moscadelli, T. M. Dame, and B. Zhang, *Astrophys. J.* 769, 15 (2013).
45. P. T. de Zeeuw, R. Hoogerwerf, J. H. J. de Bruijne, A. G. A. Brown, and A. Blaauw, *Astron. J.* 117, 354 (1999).